

# Particle dynamics and Stochastic Resonance in Periodic potentials

Shantu Saikia<sup>1\*</sup>

<sup>1</sup>*St. Anthony's College, Shillong-793001, Meghalaya, India*

(Dated: March 9, 2022)

## Abstract

We have studied the dynamics of a particle in a periodically driven underdamped periodic potential. Recent studies have reported the occurrence of Stochastic Resonance (SR) in such systems in the high frequency regime, using input energy per period of external drive as a quantifier. The particle trajectories in these systems can be in two dynamical states characterised by their definite energy and phase relation with the external drive. SR is due to the noise assisted transition of the particles between these two states. We study the role of damping on the occurrence of SR. We show that a driven underdamped periodic system exhibits SR only if the damping is below a particular limit. To explain this we study the system in the deterministic regime. The existence of the two dynamical states in the deterministic regime is dependent on the amount of damping and the amplitude of external drive. We also study the input energy distributions and phase difference of the response amplitude with the external drive as a function of the friction parameter.

PACS numbers: : 05.40.-a, 05.40. jc, 05.40.Ca

---

\*Electronic address: shantusaikia@anthonys.ac.in

## I. INTRODUCTION

Stochastic Resonance (SR) is a phenomenon exhibited by non-linear systems in which the system shows an enhanced response to an external periodic forcing in the presence of an optimal amount of noise [1–3]. Initially thought of as an explanation for the recurring ice ages on earth [1], presently SR finds lots of applications in diverse biological [4–12] and physical systems [13–17]. Extensive theoretical and experimental work has been done on SR [2, 3].

Initially considered to be a phenomenon exhibited only by bistable systems [2, 4], recently there has been some studies of non-conventional SR in monostable and multistable systems [18–36, 40, 41]. In particular SR in periodic potential systems has been of interest to researchers both in the overdamped [23–29] and underdamped limit [30–36, 40, 41].

Earlier studies have established the phenomenon of SR in periodic washboard potentials [24–31, 33]. However, the phenomenon of SR in periodic potentials without any bias has been of recent interest [32–36, 40, 41]. Though there was some controversy as to whether SR occurs in an underdamped periodic potential [32], recent studies have conclusively proved the occurrence of SR in such systems [33–36, 40, 41]. Underdamped particle motion in periodic potentials has practical relevance in understanding diverse physical phenomenon [42] such as electrical conductivity of superionic conductors [43], adatom motion on crystal surfaces [44], resistively coupled shunted junction (RCSJ) model of Josephson junctions [45] etc.

In an experimental work [34], the SR phenomenon in an underdamped periodic potential system was studied by taking a dissipative optical lattice as the spatially periodic system. They used laser fields to create the periodic potential and produce the stochastic process of optical pumping. The friction experienced by the atoms was kept low so that they exhibited underdamped motion. Using this model, Schiavoni et. al. observed the phenomenon of SR on the Brillouin propagation modes of the dissipative optical lattice. They also gave a theoretical account of their experimental findings. Zhang et.al [35] studied the mobility and diffusion of underdamped Brownian particle in a two-dimensional periodic potential. They observed that the effect of two dimensions leads to the observance of SR in the system. The output quantities like signal amplification and diffusion rate shows a peaking behaviour with temperature which otherwise is absent in the one dimensional potential.

In an earlier work, using the average input energy per period of drive and hysteresis loop area as quantifiers of SR, it was shown that the phenomenon of SR occurs in a periodically driven underdamped periodic potential in the high-frequency regime of the external forcing [36]. The phenomenon of SR was observed with a periodic potential system which was symmetric and also when an asymmetry was introduced into the system in the form of a space dependent friction coefficient. Such a spatially inhomogeneous periodic potentials system have been studied earlier to obtain particle current in the overdamped [37, 38] as well as in the underdamped [39] regime. In this work, it is shown that the particles in the system can be in two distinct dynamical states of trajectories with distinct amplitude and phase relationship with the external drive. At low temperatures, the two dynamical states are stable with fixed energies. However with the rise of temperature, transition occurs between these two states. The phenomenon of SR was attributed to the noise assisted transitions that the particles make between these two states, synchronised with the external drive. In a subsequent work [40], the role of the driving amplitude on the occurrence of SR was studied. It was shown that there is a particular range of driving amplitude for which the system exhibits the phenomenon of SR. This is because the relative stability of the two dynamical states of the particle depends on the amplitude of the external drive. Similar SR phenomenon was also observed in a bistable periodic potential and washboard potential [33]. All the above works on SR [33, 36, 40] were with Gaussian white noise. In a recent work [41], the effect of colored noise on the phenomenon of SR in the underdamped motion of a particle in a periodic potential was addressed. Colored noise was shown to affect the transitions between the two dynamical states and thus SR. Also it was observed that, as the correlation time increases, the SR peak shifts and the sharpness of the peak decreases.

In this work we study the role of damping on SR in a periodically driven underdamped periodic potential with Gaussian white noise, using the same model as in Ref. [36, 40]. We use input energy per period of external drive  $F(t)$  as a quantifier of SR. The input energy per period of external drive or the work done on the system per period of drive is calculated using the stochastic energetics formulation of Sekimoto [46]. This quantity has been found to be a good quantifier for SR in earlier studies for bistable systems [47, 50, 51] as well as periodic potentials [33, 36, 40, 41]. We show that in a driven underdamped periodic system, the amount of damping present in the medium plays a crucial role on the occurrence of SR. In such a system the particle trajectory,  $x(t) = x_0 \cos(\omega t + \phi)$ , can exist in

two definite dynamical states, with a distinct phase difference  $\phi$  with the external drive  $F(t)$ ; the low amplitude *in-phase* state, with  $\phi = \phi_1$  which is almost in phase with the external drive, and the higher amplitude, *out-of-phase* state, with  $\phi = \phi_2$ , having higher phase difference with the external drive. The *in-phase* state has lower energy associated with it and the *out-of-phase* state has higher energy. The occurrence of SR is due to the noise assisted transitions that the particles make between these two states [33, 36, 40, 41]. To explain the observed dependence of SR on damping we study the stability of the two dynamical states of trajectories with respect to the different parameters like temperature, amplitude of drive and the friction coefficient. We study the input energy distributions at different temperatures across the SR peak for various values of the friction coefficient, to characterise SR as has been done in earlier studies [33, 36, 51]. From the average response of the particle to the external drive  $\bar{x}(t) = \bar{x}_0 \cos(\omega t + \bar{\phi})$ , we calculate the average phase difference  $\bar{\phi}$  from the  $F(t) - x(t)$  hysteresis loops. We study the variation  $\bar{\phi}$  with different values of damping. The role of the average phase difference  $\bar{\phi}$  of the response amplitude  $\bar{x}(t)$  and the external forcing  $F(t)$  on SR has been explored earlier [36, 47–49].

In section II we discuss the model used. Section III contains the detailed discussion of our results while in Section IV we conclude our results.

## II. THE MODEL

In this work, we consider the underdamped motion of a particle in a periodic potential  $V(x) = -V_0 \sin(kx)$  which is symmetric in space and having a period of  $2\pi$ . The system is driven periodically by an external forcing  $F(t) = F_0 \cos(\omega t)$ . The constants  $V_0$  and  $F_0$  are the amplitudes of the potential and the driving force respectively.

The dynamics of a particle of mass  $m$  moving in a periodic potential  $V(x) = -V_0 \sin(kx)$  in a medium with friction coefficient  $\gamma$  driven by an external periodic forcing  $F(t)$ , in the presence of random fluctuations is described by the Langevin equation,

$$m \frac{d^2 x}{dt^2} = -\gamma \frac{dx}{dt} - \frac{\partial V(x)}{\partial x} + F(t) + \sqrt{\gamma T} \xi(t). \quad (2.1)$$

In the above equation, the temperature  $T$  is in units of the Boltzmann constant  $k_B$ .  $\xi(t)$  represents the random fluctuations in the system satisfying the statistics:  $\langle \xi(t) \rangle = 0$ , and  $\langle \xi(t) \xi(t') \rangle = 2\delta(t - t')$ . The above equation can be written in dimensionless units

by setting  $m = 1$ ,  $V_0 = 1$ ,  $k = 1$ . Using the same symbols for the reduced variables, the dimensionless form of the Langevin equation becomes

$$\frac{d^2x}{dt^2} = -\gamma \frac{dx}{dt} + \cos x + F(t) + \sqrt{\gamma T} \xi(t). \quad (2.2)$$

In the above equation too,  $\xi(t)$  obeys the same statistics as before. For studying the particle dynamics in the deterministic regime,  $T$  is set equal to 0.

### III. NUMERICAL RESULTS

The underdamped Langevin's equation (Eq. 2) is solved numerically using  $2^{nd}$  order Heun's method [54], by treating it as an initial value problem. We take an integration-time step  $\Delta t = 0.001$ . In the deterministic regime [52] and also in the low temperature, low amplitude regime [36], the dynamics of the particle is sensitively dependent on the initial conditions,  $x(0) = x(t=0)$  and  $v(0) = v(t=0)$ . So for physically relevant results, ensemble averaging is done over an ensemble of 100 particles starting with different initial positions,  $x_i(0)$ ,  $i = 1, 2, \dots, 100$ , taken from a uniformly spaced grid between the two consecutive peaks of the periodic potential and initial velocity  $v = 0$  [53].

The input energy, or work done on the system per period of the external drive,  $E_i$ , is calculated using the stochastic energetics formulation of Sekimoto [46] as

$$E_i(t_0, t_0 + \tau) = \int_{t_0}^{t_0 + \tau} \frac{\partial U(x(t), t)}{\partial t} dt, \quad (3.1)$$

where,  $\tau$  is the period of the external drive, the potential  $U(x(t), t) = V(x) - xF(t)$ , and  $V(x) = -\sin(x)$ ,  $F(t) = F_0 \cos(\omega t)$ . For our calculations we consider  $F_0 = 0.2$  and  $\tau = 8.0$  unless otherwise stated. The value of  $\tau = 8.0$  is in the high frequency regime close to the natural frequency at the bottom of the potential wells.

To find the average input energy per period of external drive  $\langle \overline{E_i} \rangle$ , averaging is first done over all the periods of one trajectory as

$$\overline{E_i} = \frac{\sum_{n=N_t}^{N_f} E_{in}}{N_f - N_t} \quad (3.2)$$

The number of periods,  $N_f$ , taken in a trajectory ranges between  $10^5$  to  $10^7$ , as required.  $N_t$  is the initial number of transients which are removed.  $\langle \overline{E_i} \rangle$  is then calculated by averaging  $\overline{E_i}$  over all the trajectories.

The results of our numerical calculations are presented in the following sections.

### A. Input energy versus temperature for different damping

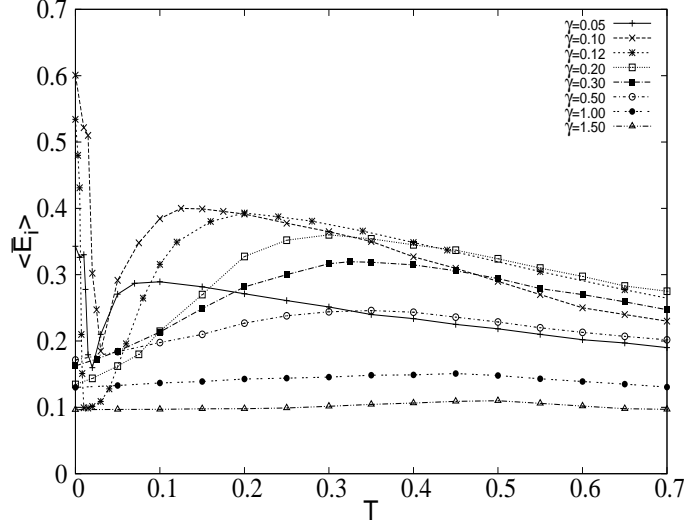


FIG. 1: Plot of  $\langle \overline{E}_i \rangle$  versus  $T$ , for different values of the friction coefficient  $\gamma$ ;  $F_0 = 0.2$  and  $\tau = 8$ .

Fig.1. shows the main result of our work. The input energy per period or the work done per period over external drive  $\langle \overline{E}_i \rangle$  is plotted versus the temperature  $T$  for different values of the friction coefficient  $\gamma$  in the medium. It is observed that for lower values of  $\gamma$ , the  $\langle \overline{E}_i \rangle$  versus  $T$  curve shows a peaking behaviour which is a signature of SR [33, 36, 40, 41]. However as  $\gamma$  increases, the phenomenon of SR becomes negligible and is almost absent for  $\gamma = 1.50$ . Also the sharpness of resonance decreases with the increase in the value of  $\gamma$ .

There is a significant change in the nature of the  $\langle \overline{E}_i \rangle$  versus  $T$  curves at lower temperatures as  $\gamma$  changes. For  $\gamma = 0.05, 0.10$  and  $0.12$ , as temperature increases,  $\langle \overline{E}_i \rangle$  attains a minimum and then increases to attain a peak at an intermediate  $T$ . However for  $\gamma = 0.2, 0.3, 0.5$  and  $1.0$  the minima observed at lower  $T$  is missing.

### B. Particle dynamics in different parameter regimes

To explain this observed behaviour, we study the particle dynamics in the deterministic regime. Fig. 2 shows the plot of average input energy per period in a trajectory,  $\overline{E}_i$  versus the initial position  $x(0)$  for different values of  $\gamma$ . For lesser damping, in the deterministic

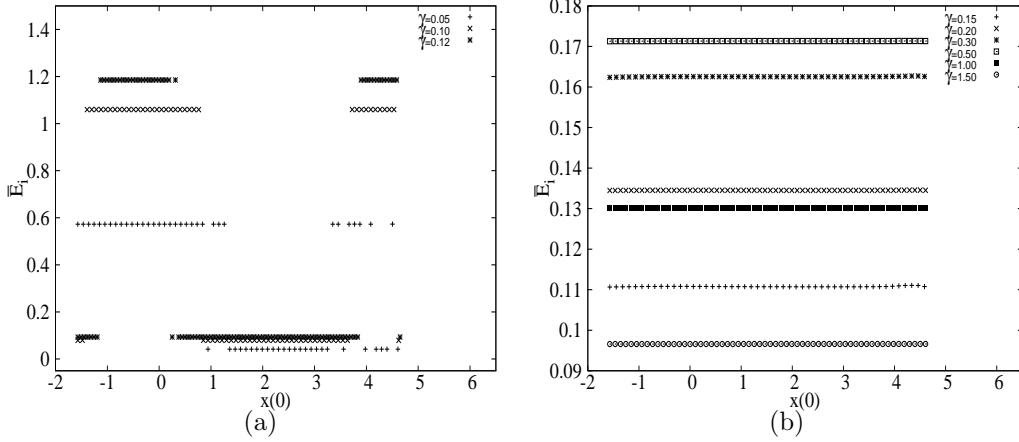


FIG. 2: Plot of  $\overline{E}_i$  versus  $x(0)$  for different values of the friction coefficient  $\gamma$ ;  $F_0 = 0.2$  and  $\tau = 8.0$ .

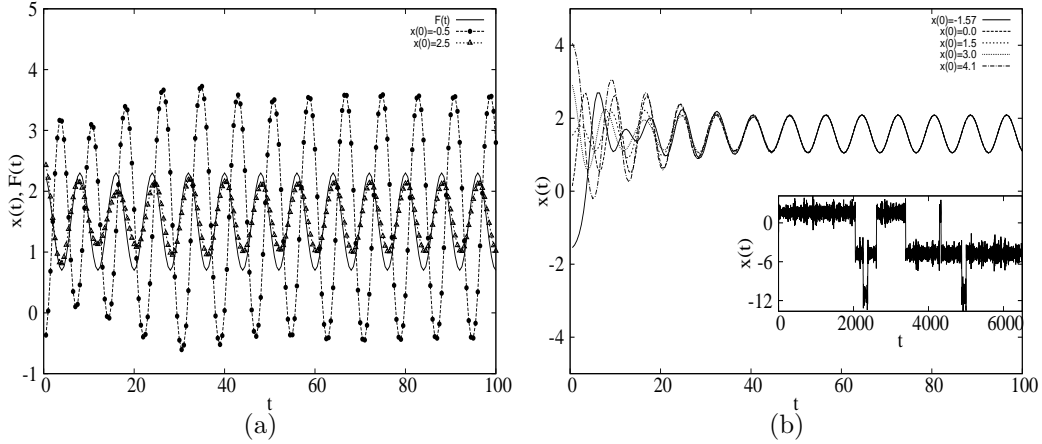


FIG. 3: Plot of  $x(t)$  and  $F(t)$  for different  $x(0)$  with  $T = 0$  for  $\gamma = 0.1$ (a) and for  $\gamma = 0.2$  (b). Inset of (b) shows plot of  $x(t)$  for  $\gamma = 0.2$  with  $T = 0.2$ ;  $x(0) = -1.57$ ,  $F_0 = 0.2$ ,  $\tau = 8.0$ .

limit (and also for lower temperatures [36]), the particles can exist in two distinct dynamical states of trajectories depending on the initial positions  $x(0)$  (Fig. 2a). These dynamical states are distinctly characterised by the phase difference  $\phi$  between the particle trajectory  $x(t) = x_0 \cos(\omega t + \phi)$  and the external periodic drive  $F(t) = F_0 \cos(\omega t)$ . The *in-phase* has lower amplitude and hence lesser energy and while the *out-of-phase* state has higher amplitude and hence higher energy.

Fig. 3a shows the in-phase state of trajectory with  $x(0) = 2.5$  and the high amplitude out-of-phase trajectory with  $x(0) = 0.5$  in the deterministic limit ( $T = 0$ ). The presence of the high energy state leads to higher average input energy at  $T = 0$  or at low  $T$ . As  $T$  increases, all the particles come down to the low energy state [36]. Thereafter, with

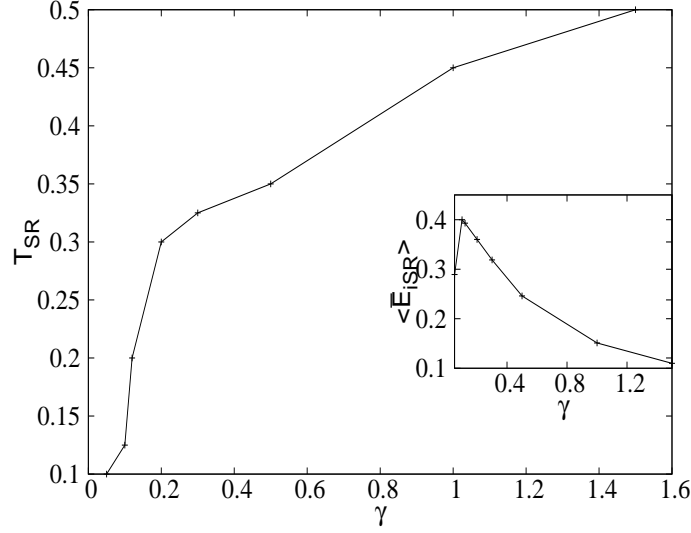


FIG. 4: Plot of  $T_{SR}$  versus  $\gamma$ . Inset shows the variation of  $\langle \overline{E}_{iSR} \rangle$  with  $\gamma$ ;  $F_0 = 0.2$  and  $\tau = 8$

the rise of temperature the particles make transitions between the two states. The average input energy peaks at a value of  $T$ , where optimum transitions occur, synchronised with the external drive. For higher damping, all the particles for a particular  $\gamma$  value, are in the same energy state at  $T = 0$  (and also at lower  $T$ ), irrespective of the initial conditions (Fig. 2b).  $\overline{E}_i$  comparatively lower than the high energy states of the low damping regime. A look into the particle trajectories reveals that when damping is high, the particles loses sensitivity to the initial conditions and all the particles after sometime goes to the same state of motion with lesser amplitude and hence energy (main Fig. 3b). This leads to low  $\langle \overline{E}_i \rangle$  at  $T = 0$  or low  $T$ . Though at low  $T$ , the two dynamical states are not there for higher damping, as  $T$  increases, the particle makes transitions between a low amplitude and high amplitude motion (Inset of Fig. 3b). The peaking of  $\langle \overline{E}_i \rangle$  at an optimum  $T$  is therefore apparently due to the synchronised transitions between the two types of particle motion.

The value of temperature  $T = T_{SR}$  at which the average input energy  $\langle \overline{E}_i \rangle$  peaks, increases as the damping increases (Fig. 4). Significantly, the value of average input energy at the peak of the SR curve, is maximum for an optimum value of damping (Inset of Fig. 4).

The observed shift in the SR peak to higher  $T$  for higher  $\gamma$  is due to the fact that when damping is high, the optimum synchronisation of transition between the two dynamical states of the particle occurs at higher values of  $T$ .

At still higher values of  $\gamma$ , the particle motion reaches the overdamped regime, leading to the absence of the peaking behaviour.



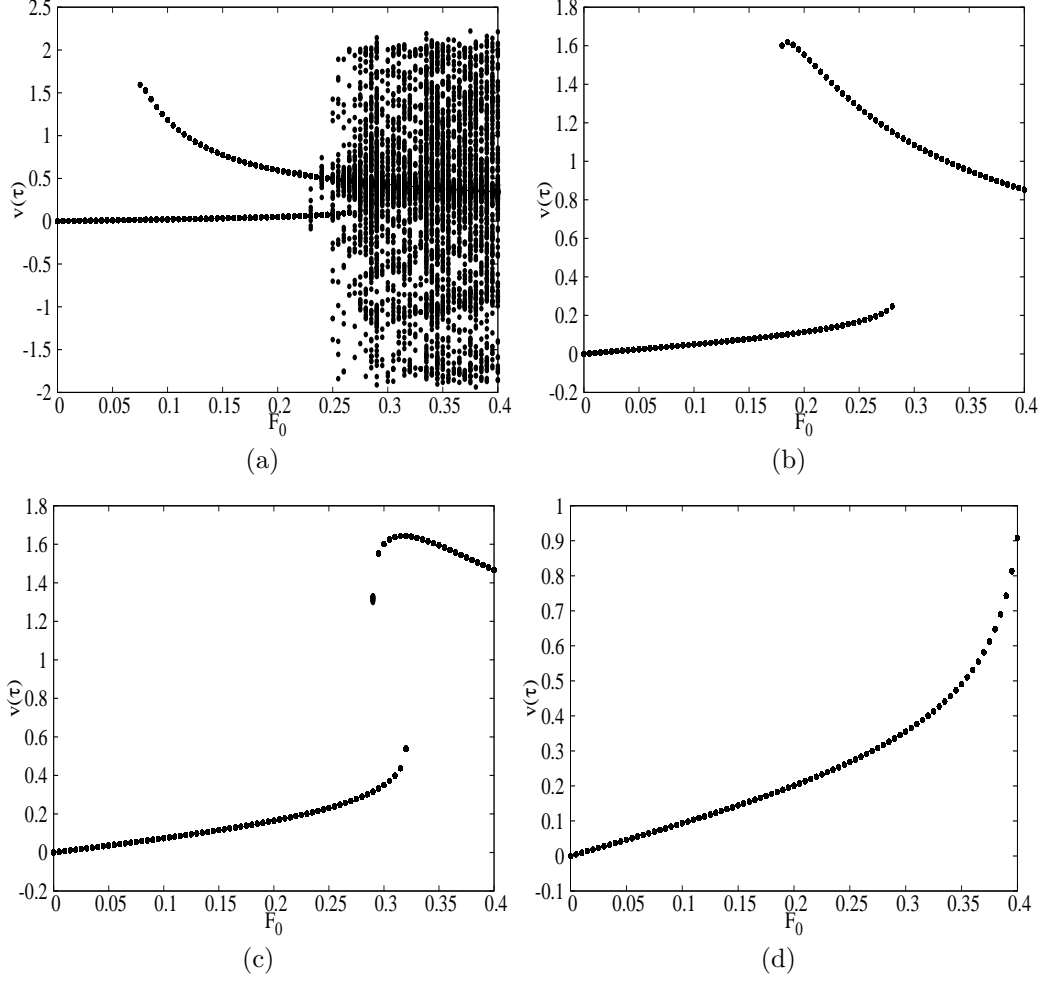


FIG. 5: Bifurcation diagrams for different values of  $\gamma$  in the deterministic limit ( $T = 0$ );  $\gamma = 0.05$  (a),  $\gamma = 0.12$  (b),  $\gamma = 0.2$  (c) and  $\gamma = 0.3$  (d);  $\tau = 8.0$ .

### C. Bifurcation diagrams

Fig. 5 shows the bifurcation diagram in the deterministic regime for different values of damping. These are obtained by recording the particle velocity  $v(T_p)$  at times  $T_p = \tau$  equal to the period of the external drive and plotting them as a function of a control parameter, here  $F_0$ , the amplitude of the external drive [52]. For the value of amplitude  $F = 0.2$ , considered for Fig. 1, the bifurcation diagram clearly shows the existence of two regular trajectories - one with higher velocity and the other with lesser velocity for  $\gamma = 0.05, 0.10, 0.12$ .

This shows that the two dynamical states accessible to the particle for lower damping can be associated with the regular trajectories in the deterministic regime. Incidentally, for  $\gamma = 0.12$ , for the range of  $0.18 \leq F_0 \leq 0.28$ , two regular trajectories exists and it corresponds

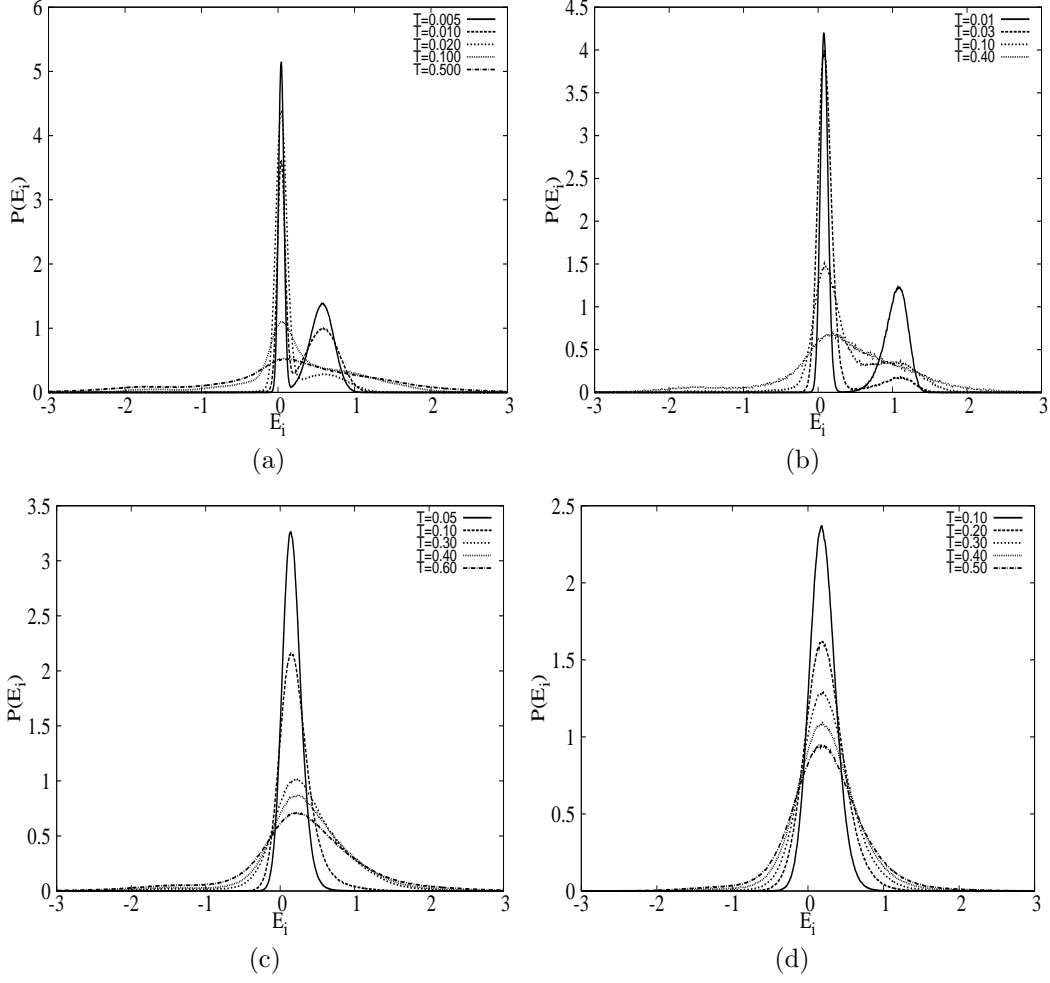


FIG. 6: Plot of  $P(E_i)$  at different values of  $T = 0$  for  $\gamma = 0.05$  (a),  $\gamma = 0.1$  (b),  $\gamma = 0.2$  (c) and  $\gamma = 0.5$  (d);  $\tau = 8.0$ ,  $F_0 = 0.2$ .

exactly to the range of  $F_0$  in which SR behaviour is observed in Ref. [40]. The presence (or absence) of different number of dynamical states of trajectories in the deterministic limit or for lower temperatures obviously depends on the value of friction coefficient  $\gamma$  and the amplitude of external drive  $F_0$  under consideration.

#### D. Input energy distributions

Fig. 6 shows the input energy distributions for the different  $\gamma$  values considered in Fig. 1 corresponding to different temperatures. The nature of the input energy distributions have earlier been successfully used to understand the nature of the SR behaviour [36, 51].

The bimodal nature of the distributions at low temperatures for  $\gamma = 0.05, 0.1$  and  $0.12$

clearly shows the existence of the high energy and low energy dynamical states. As temperature rises the input energy distributions becomes asymmetrical, with highest asymmetry at temperatures corresponding to the SR peak. For very high temperatures, the input energy distributions again becomes symmetrical about the mean value. However, for values of  $\gamma$  for which SR behavior is absent,  $\gamma = 1.5$ , the input energy distributions are almost symmetrical for all values of temperature.

### E. Variation of $\bar{\phi}$ vis a vis $\langle \bar{E}_i \rangle$ with $\gamma$

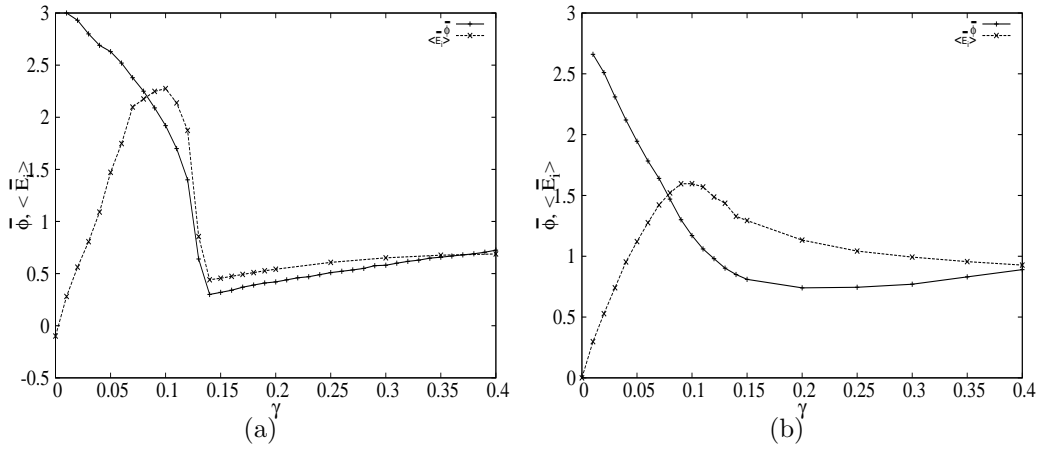


FIG. 7: Plot of  $\bar{\phi}$  and  $\langle \bar{E}_i \rangle$  (increased by a factor of 4.0) versus  $\gamma$ , for  $T = 0.0$  (a) and  $T = 0.15$  (b);  $F_0 = 0.2$  and  $\tau = 8$ .

In this section we study the variation of the phase difference  $\bar{\phi}$  between the external drive  $F(t)$  and the average particle response  $x(t) = \bar{x}_0 \cos(\omega t + \bar{\phi})$ , and  $\langle \bar{E}_i \rangle$  with  $\gamma$ . It is seen that in the deterministic limit (Fig. 7a) and also for a finite temperature (Fig. 7b),  $\bar{\phi}$  and  $\langle \bar{E}_i \rangle$  shows a non monotonic behaviour with the change of  $\gamma$ . With the increase of  $\gamma$  from lower value,  $\langle \bar{E}_i \rangle$  shows a peaking behaviour with  $\gamma$ , while  $\bar{\phi}$  decreases showing an inflection point around the value of  $\gamma$  where  $\langle \bar{E}_i \rangle$  peaks. In Ref. [33, 36, 40, 48]  $\bar{\phi}$  was shown to have an inflection point at the peak of SR. We observe that even with the variation of  $\gamma$ ,  $\langle \bar{E}_i \rangle$ , exhibits a peaking with an associated inflection point in the phase lag.

In the deterministic case (Fig. 7a), as  $\gamma$  changes, the average input energy after attaining a peak again goes to a minimum. The value of  $\gamma$  at the minima corresponds to the level of damping at which the two dynamical states of trajectories ceases to exist (as discussed above in the explanation of Fig. 2).

#### IV. DISCUSSION AND CONCLUSION

An underdamped periodic potential system exhibits SR when driven with a high frequency drive close to the natural frequency at the bottom of the potential wells. SR with average input energy per period  $\langle \overline{E_i} \rangle$  as a quantifier, is found to occur only in the low damping regime. The transitions between the two definite states of the particle trajectories, characterised by their phase difference with the external drive, offers a possible explanation for the occurrence of SR [33, 36, 40, 41]. The existence of these two states are found to be dependent on the choice of the friction coefficient  $\gamma$  and the amplitude of drive  $F_0$ . For  $F_0 = 0.2$  considered here, in the low damping regime,  $0 < \gamma < 0.14$ , the two dynamical states exists at  $T = 0$  or at lower temperatures. However for  $0.14 < \gamma < 1.5$ , though, only a single dynamical state of trajectory exists near about the deterministic limit, SR behaviour is observed. This is because, with the rise of temperature, the particle trajectories alternates between a high amplitude and low amplitude regime. Synchronised transitions between these two regimes at an optimum temperature gives rise to the peak in  $\langle \overline{E_i} \rangle$ . The percentage of time that the particle spends in the high amplitude and low amplitude regime and its relation to SR needs to be further explored. As with temperature, the average input energy also shows a peaking behaviour with the friction coefficient  $\Gamma$ . The phase difference  $\bar{\phi}$  between  $F(t)$  and  $\bar{x}(t)$  has an inflection point exactly at the  $\gamma$  value corresponding to the peak of  $\langle \overline{E_i} \rangle$  vs  $\gamma$  curve. So the criteria of the presence of an inflection in  $\bar{\phi}$  is not exclusive only for SR peaks [33, 36, 40, 48].

- 
- [1] R. Benzi, A. Sutera, and A. Vulpiani J. Phys. A 14, L453 (1981).
  - [2] L. Gammaitoni, P. Hänggi, P. Jung, and F. Marchesoni, Rev. Mod. Phys. 70, 223 (1998).
  - [3] T. Wellens, V. Shatokhin, and A. Buchleitner, Rep. Prog. Phys. 67, 45 (2004).
  - [4] K. Wiesenfeld, and F. Moss, Nature 373, 33 (1995).
  - [5] J. Maddox, Nature (London) 369, 271 (1994).
  - [6] P. Hanggi, ChemPhysChem, 3, 285 (2002).
  - [7] P.K. Ghosh, B.C. Bag, D.S. Ray, Phys. Rev. E 75, 032101 (2007).
  - [8] J.K. Douglass, L. Wilkens, E. Pantazelou, and F. Moss, Nature 365, 337 (1993).
  - [9] J.J. Collins, T.T. Imhoff, and P. Grigg, J. Neurophysiology 76, 642 (1996).

- [10] B.J. Gluckman, T.I. Netoff, E.J. Neel, W.L. Ditto, M.L. Spano, and S.J. Schiff, Phys. Rev. Lett. 77, 4098 (1996).
- [11] E. Simonotto, M. Riani, C. Seife, M. Roberts, J. Twitty, and F. Moss, Phys. Rev. Lett. 78, 1186 (1997).
- [12] S. Ikemoto, F.D. Libera, K. Hosodo, Phys. Rev. E, 85, 021905 (2012).
- [13] S. Fauve, and F. Heslot, Phys. Lett. A 97, 5 (1983).
- [14] R.N. Mantegna, and B. Spagnolo, Phys. Rev. E 49, R1792 (1994).
- [15] K. Murali, S. Sinha, W.L. Ditto, A.R. Bulsara, Phys. Rev. Lett. 102, 104101 (2009).
- [16] B. McNamara, K. Wiesenfeld, and R. Roy, Phys. Rev. Lett. 60, 2626 (1988).
- [17] R.L. Badzey, and P. Mohanty, Nature 437, 995 (2005).
- [18] N.G. Stocks, P.V.E. McClintock, and S.M. Soskin, Europhys. Lett. 21, 395 (1993); N.G. Stocks, N.D. Stein, and P.V.E. McClintock, J. Phys. A: Math. Gen. 26, L385 (1993).
- [19] M.I. Dykman, D.G. Luchinsky, R. Mannella, P.V.E. McClintock, N.D. Stein, and N.G. Stocks J. Stat. Phys. 70, 479 (1993).
- [20] S. Arathi and S. Rajasekar, Physica Scripta, Vol. 84, No. 6, 065011 (2011).
- [21] K. Wiesenfeld, D. Pierson, E. Pantazelou, C. Dannes and F. Moss, Phys. Rev. Lett. 72, 2125 (1994).
- [22] I.Kh. Kaufman, D.G. Luchinsky, P.V.E. McClintock, S.M. Soskin, and N.D. Stein, Phys. Lett. A 220, 219 (1996).
- [23] N. Lin-Ru, G.Yu-Lan, M. Dong-Cheng, Chin. Phys. Lett. Vol. 26, No. 10 (2009) 100505.
- [24] D. Dan, M. C. Mahato and A. M. Jayannavar, Phys. Lett. A 258, 217(1999), Phys. Rev. E 60, 6421 (1999).
- [25] L. Fronzoni and R. Mannella, J. Stat. Phys. 70, 501 (1993).
- [26] G. Hu, Phys. Lett. A, Vol. 174, Issue 3 (1993), 247.
- [27] J. M. Cassado, J. J. Mejias and M. Morillo, Phys. Lett. A 365, 366 (1995).
- [28] M. Gitterman, I. B. Khalfin and B. Ya. Shapiro, Phys. Lett. A, 339, 340 (1994).
- [29] J. D. Bao, Phys. Rev. E 62, 4606 (2000); Phys. Lett. A, Vol. 265, Issue 4, 244 (2000).
- [30] F. Marchesoni, Phys. Lett. A 231, 61 (1997).
- [31] J. Kallunki, M. Dube and T. Ala-Nissila, J. Phys. Cond. Mat. 11, 9841 (1999).
- [32] Y.W. Kim, W. Sung, Phys. Rev. E 57 (1998) R6237.
- [33] W.L. Reenbohn, S.S. Pohlong, M.C. Mangal, Phys. Rev. E 85 (2012) 031144.

- [34] M. Schiavoni, F.-R. Carminati, L. Sanchez-Palencia, F. Renzoni and G. Grynberg, Eur. Phys. Lett., Vol. 59, No. 4, 493(2002).
- [35] X. Zhang, J. Bao, Surface Science, Vol. 540, Issue 1, (2003) 145.
- [36] S. Saikia, A.M. Jayannavar, M.C. Mahato, Phys. Rev. E 83 (2011) 061121.
- [37] M. C. Mahato, T. P. Pareek and A. M. Jayannavar, Int. J. of Mod. Phys. B10, 3857(1996).
- [38] D. Dan, A. M. Jayannavar and M. C. Mahato, Int. J. of Mod. Phys. B14, 1585(2000).
- [39] S. Saikia and M. C. Mahato, J. Phys.: Condens. Matter 21 (2009) 175409.
- [40] W. L. Reenbohn, M. C. Mangal, Phys. Rev. E 88, 032143 (2013).
- [41] K. Liu, Y. Jin, Physica A 392 (2013) 52835288.
- [42] H. Risken, *The Fokker-Planck Equation*(Springer, Berlin, 1989).
- [43] P. Fulde, L. Pieternero, W. R. Schneider and S. Strassler, Phys. Rev. Lett. 35, 1776 (1975); A. Asaklil, Y. Boughaleb, M. Mazroui, M. Chhib and L. El Arroum , Solid State Ionics 159, 331 (2003).
- [44] A. M. Lacasta, J. M. Sancho, A. H. Romero, I. M. Sokolov and K. Lindenberg, Phys. Rev. E, 70, 051104 (2004); A. P. Graha, F. Hoffmann, J. P. Toennies, L. Y. Chen and S. C. Ying, Phys. Rev. B 56, 10567 (1997); D. C. Senft and E. Ehrlich, Phys. Rev. Lett. 74, 294 (1995).
- [45] C. M. Falco, Am. J. Phys. 44, 733 (1976); A. Barone and G. Paterno, Physics and Applications of the Josephson Effect (Wiley, Newyork, 1982).
- [46] K. Sekimoto, J. Phys. Soc. Jpn. 66, 1234 (1997).
- [47] T. Iwai, Physica a 300, 300 (2001); T. Iwai, J. Phys. Soc. Jpn. 70, 353 (2001).
- [48] L. Gammaitoni, F. Marchesoni, M. Martinelli, L. Pardi and S. Santucci, Phys. Lett. A 158, 449 (1991).
- [49] M. I. Dykman, R. Mannella, P. V. E. McClintock and N. G. Stocks, Phys. Rev. Lett. 68, 2985 (1992); L. Gammaitoni and F. Marchesoni, Phys. Rev. Lett. 70, 873 (1993), M. I. Dykman, R. Manella, P. V. E. McClintock and N. G. Stocks, Phys. Rev. Lett. 70, 874 (1993).
- [50] D. Dan, A. M. Jayannavar, Physica A 345, 404 (2005).
- [51] S. Saikia, R. Roy, A. M. Jayannavar, Phys. Lett. A 369, 367 (2001)
- [52] S. Saikia, and M.C. Mahato, Physica A 389, 4052 (2010), and references therein.
- [53] J. L. Mateos, Phys. Rev. Lett. 84, 258 (2000).
- [54] R. Mannella, A Gentle Introduction to the Integration of Stochastic Differential Equations. In : *Stochastic Processes in Physics, Chemistry, and Biology*. Edited by J. A. Freund and T.

Pöschel, Lecture Notes in Physics, vol. 557, 353. Springer, Berlin, 2000.

[55] J. L. Mateos, Phys. Rev. Lett., 84, 258 (2000).